RESEARCH ARTICLE

Design of Frequency-Reconfigurable Branch-Line Crossover Using Rectangular Dielectric Channels

RUSAN KUMAR BARIK [1], (Member, IEEE), SLAWOMIR KOZIEL [1,2], (Fellow, IEEE), AND EIRÍKUR BERNHARÐSSON[1]

[1]Department of Engineering, Reykjavik University, 102 Reykjavik, Iceland
[2]Faculty of Electronics, Telecommunications and Informatics, Gdańsk University of Technology, 80-233 Gdańsk, Poland

Corresponding author: Slawomir Koziel (koziel@ru.is)

ABSTRACT This paper presents an efficient yet straightforward passive reconfiguration technique to tune the operating frequency of a branch-line crossover (BLCO). The underlying principle is to fill rectangular dielectric channels (RDCs) prepared beforehand with either air or materials of different relative permittivity. Two configurations (one RDC and three RDCs in each arm) of the branch-line crossover are employed to estimate the tunability range of the operating frequency. The introduction of RDCs packed with different materials in the branch lines modifies the effective permittivity of the dielectric medium, resulting in an alteration of the operating frequency. The size and the positions of the RDCs are optimized using full-wave electromagnetic simulations to achieve maximum tunability range while ensuring reasonable bandwidth. A lumped circuit model (LCM) is developed to analyze the working principle of the proposed technique. To validate computational models, two prototypes of the branch-line crossover are realized, fabricated, and experimentally demonstrated. The first BLCO packed with seven RDCs exhibits a frequency tuning range of 15.8%, whereas the second prototype filled with twenty-one RDCs features a tuning range of 36.9%.

INDEX TERMS Branch-line crossover, reconfigurable, dielectric-loaded.

I. INTRODUCTION

Smaller gadgets featuring more intricate designs have now become possible due to rapid advancements in wireless communication technology. It is often essential for two RF traces to cross each other on a printed circuit board (PCB) while retaining a high level of isolation due to the reduced size of the device. A microwave crossover is a four-port device that enables the joining of two transmission lines while maintaining the necessary isolation, thereby ensuring proper operation of the system. Crossovers are often utilized in Butler matrices employed in feeding networks of antenna arrays. Crossovers were initially built using three-dimensional (3D) structures including bond wires, via holes, underpasses, and air bridges [1], [2], [3]. These designs exhibited high return loss in the passband in addition to fabrication problems.

To address these issues, branch line structures have been proposed to realize planar crossovers with smaller footprint areas, wideband, and multi-band responses [4], [5], [6], [7], [8], [9], [10], [11], [12], [13], [14], [15], [16], [17], [18], [19], [20], [21], [22].

Compact size, broad bandwidth, and harmonic suppression are the three most typical requirements of modern wireless technology. Accordingly, planar branch-line crossovers that are small, enable harmonic suppression and wideband operation, have been designed [4], [5], [6], [7], [8], [9], [10], [11], [12], [13], [14], [15], [16], [17]. Based on the branch-line layouts, nonstandard planar crossovers have been constructed in [4]. Multi-section branch-line couplers have been examined in [5] in order to realize a planar crossover. A truncated microstrip patch has been used to create a planar crossover for wideband applications [6]. In [7], a compact planar crossover for broadband applications was achieved by cascading branch-line

The associate editor coordinating the review of this manuscript and approving it for publication was Wenjie Feng.

couplers. Microstrip-line to ridge-waveguide transition has been used to realize a crossover featuring wideband and high isolation responses [8]. The 5-, 6-, and 7-section-based planar crossovers have been examined in [9]. Using coupled lines, a compact filtering crossover has been achieved in [10]. By using multi-section branch lines with open stubs, a miniature crossover has been constructed in [11]. In [12], a miniature crossover was designed using three-section metamaterial lines. By incorporating multi-section branch lines with open stubs, a miniature crossover has been proposed in [13]. In [14], a crossover with wideband and harmonic suppression has been reported using multi-section microstrip lines with adjustable impedances. The above-designed crossovers exclusively work in a single frequency band, which restricts their use in systems that support many communication standards.

To support multiple standards in current wireless technology, several configurations have been developed to implement multi-band crossovers [15], [16], [17], [18], [19], [20], [21], [22]. In [15], a dual-band crossover has been designed by employing right/left-handed transmission lines. In [16], a two-section branch-line configuration has been analyzed for the realization of a dual-band crossover. A two-section branch-line configuration with an H-shaped line has been applied to develop a miniature crossover for dual-frequency application [17]. In [18], a planar dual-band crossover with high isolation has been constructed using open-ended coupled lines. In [19], a dual-band crossover has been designed by using a dumbbell-shaped resonator. In [20], a triple-band planar crossover has been realized based on the multi-band transmission lines. In [21], a cross-shaped line has been employed for the design of a dual-band crossover.

Crossovers such as those mentioned earlier are only suitable for fixed-frequency applications. However, in order to save the cost and reduce the size, software-defined radio and cognitive radio mandate that current transceiver systems be capable of being customized for tunable frequencies and different communication standards. Consequently, reconfigurable microwave passive components have been attracting considerable attention. Reconfigurability of components has been achieved by employing lumped components (p-i-n diodes or varactors) and electro-mechanical systems (MEMS). These techniques offer fast switching speeds, high-bandwidth operation, and high-quality factors, but exhibit major drawbacks such as low power-handling levels and lack of compatibility with flexible solutions required for wearable components. Therefore, liquid or solid dielectrics have been employed for the realization of tunable microwave devices [22], [23], [24], [25], [26], [27], [28], [29], [30], [31], [32], [33], [34]. Liquid dielectrics are passive and mechanically-based, highly linear, and flexible, which makes them excellent choices for high-power and wearable devices. In addition, this approach provides a wide frequency tuning range, low insertion loss, and easy fabrication as compared to diodes and MEMS methods. Recently, fluidic channels have

been applied for the construction of tunable microwave filters [22], [23], [24], [25], [26], [27], tunable frequency-selective surfaces [28], [29], and tunable antennas [30], [31], [32]. In [33], a substrate-integrated waveguide (SIW) slot antenna has been designed based on a solid dielectric rod. In [34], a miniaturized SIW-based filter with frequency tunability has been designed by applying magnetized ferrite substrate. In [35], a reconfigurable antenna has been realized using a falcate patch and an L-shaped probe. In [36], a multilayer dielectric antenna has been constructed based on the multiple dielectric stacks.

Varactor diodes and tunable capacitors have been recently used to implement a tunable planar crossover [38]. The tuning range of this device is from 1.29 GHz to 2.06 GHz. Reference [39] describes the construction of a tunable crossover based on half-mode substrate-integrated waveguides (HMSIW). Three adjustable capacitors are used between the HMSIWs to tune the operating frequency. Tunability of these circuits was made possible by semiconductor devices, which have a number of deficiencies, as discussed earlier. An alternative is to employ solid dielectric channels, which is a solution suitable for the realization of planar tunable crossovers, investigated in this work.

This article presents a novel passive reconfigurable technique to tune the operating frequency of branch-line crossovers. Rectangular channels are created by milling the transmission line of the crossover. They are packed with dielectric materials/air to achieve frequency tunability. Two models (seven and twenty-one dielectric channels) have been chosen to study the tenability properties. Filling the channels with dielectric material or air alters the effective permittivity of the dielectric medium, resulting in operating frequency shifts. To obtain maximum tunability, the position and dimension of the dielectric channels are optimized using CST Microwave Studio. A lumped-circuit model is developed to explain the working principle of the proposed crossover. For validation, two prototypes of the branch-line crossovers are developed, fabricated, and tested. Experimental results demonstrate the achievable tunability range of up to thirty percent, which is in agreement with simulation-based predictions.

II. DESIGN PROCEDURE

This section describes the proposed branch-line crossover (BLCO) configuration and the formation of dielectric channels. Subsequently, the position and dimension of the channels are optimized using a full-wave simulator. The channels are filled with different dielectric materials to obtain frequency tunability. To validate the proposed idea, a lumped circuit model (LCM) is constructed for the proposed tunable BLCO and analyzed, along with the full-wave EM simulation. The experimental demonstration and comparative analysis of state-of-the-art BLCO prototypes will be presented in Section III.
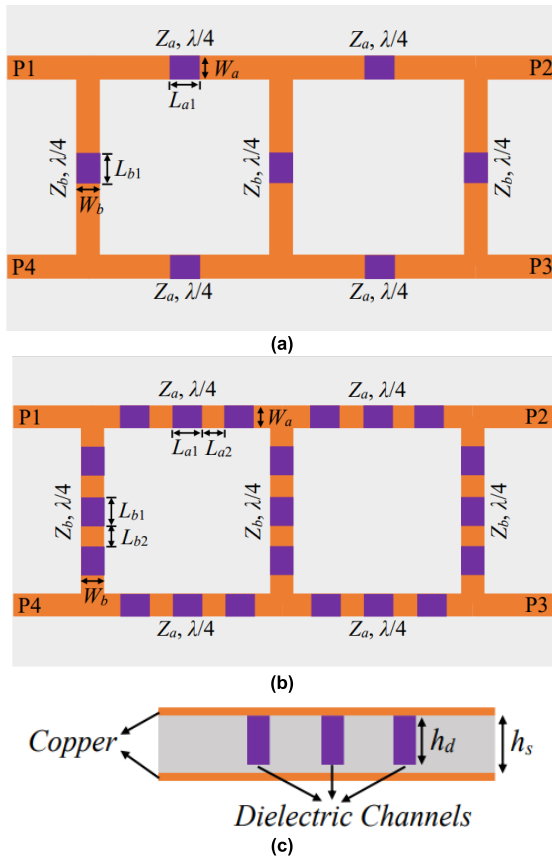
FIGURE 1. Schematic of the proposed reconfigurable branch-line crossovers: (a) a version with seven RDCs, (b) a version with 21 RDCs, (c) cross-section view of the RDC geometry. Final dimensions: $L_{a1} = 22$, $L_{a2} = 22$, $W_a = 22$, $L_{b1} = 22$, $L_{b2} = 22$, $W_b = 22$, $h_d = 1.32$, $h_s = 1.52$. (Units: Millimeters).

A. ANALYSIS OF THE PROPOSED TUNABLE BLCO

Figure 1 illustrates the layout of the proposed reconfigurable branch-line crossovers (BLCO), and the close-up view of the dielectric channels. The schematics of BLCO with 7 and 21 rectangular dielectric channels (RDCs) are shown in Figs. 1(a) and 1(b), respectively. Initially, a conventional BLCO working at 1.8 GHz is designed using seven $\lambda/4$ transmission lines with the characteristic impedance of $Z_a = Z_b = 50\Omega$.

The EM-simulated S-parameters of the conventional BLCO are shown in Fig. 2. It is found that the insertion and return losses are below 0.3 dB and 25 dB, respectively. In addition, the isolation is greater than 25 dB. The BLCO was realized using Roger's AD250C material of thickness $h_s = 1.524$ mm, $\varepsilon_r = 2.5$, and tan $\delta = 0.0014$. The proposed tunable BLCOs are developed by inserting rectangular dielectric channels. The dielectric channels are filled with air and dielectric materials to obtain operating frequency tunability.

Since the BLCO is loaded with rectangular dielectric channels, its operating frequency depends on the relative permittivity and dimension of the channels. It is challenging to mechanically adjust the dimension of the channels after
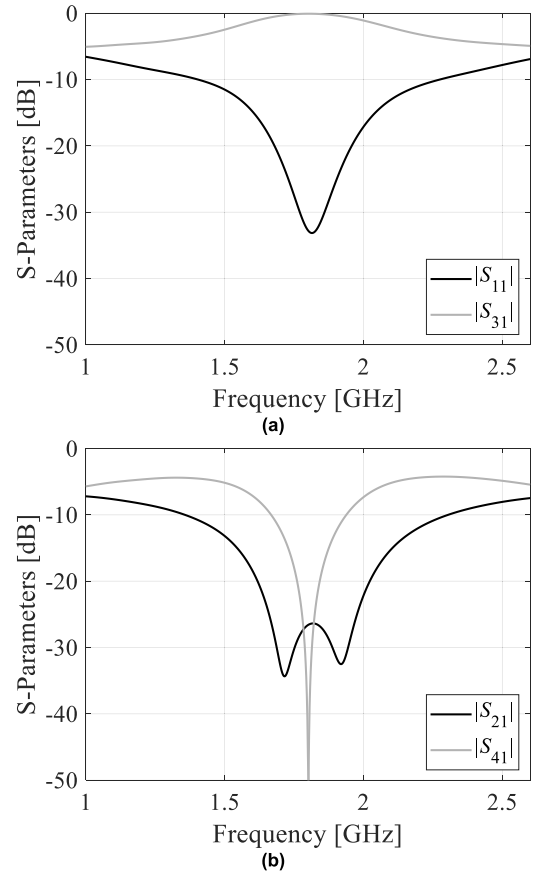

FIGURE 2. S-parameters of the conventional branch-line crossover: (a) $|S_{11}|$ and $|S_{31}|$, (b) $|S_{21}|$ and $|S_{41}|$.

manufacturing because doing so will alter the physical size of the BLCO. Therefore, it is simpler to insert various dielectric materials into the air holes in order to obtain tunability. Altering the frequency is a result of the difference in relative permittivity of the substrate and the dielectric channels. The operating frequency shifts upward when all channels are filled with air, whereas it shifts downward when all channels are filled with dielectric materials.

B. ANALYSIS OF THE BLCO WITH SEVEN RDC

The schematic of the BLCO with seven rectangular dielectric channels (RDCs) has been shown in Fig. 1(a). A rectangular dielectric channel with dimensions $L_{a1} \times W_a$ is milled on each arm of the BLCO, with a total of seven RDCs. The width of the RDCs remains the same as that of the arms. The RDCs have the same height of h_d that is less than the height of the substrate, resulting in a thin layer of the substrate to accommodate the chosen dielectric material and to keep the integrity of the ground plane intact.

The RDCs are filled with dielectric materials and air to obtain frequency tunability. In this study, we have considered Roger's RO4360G2 ($\varepsilon_r = 6.02$) and RO3010 ($\varepsilon_r = 10.2$) dielectric materials to fill the channels. The operating frequency moved to the lower value by loading the RO4360G2 and RO3010 due to the difference in relative permittivity.
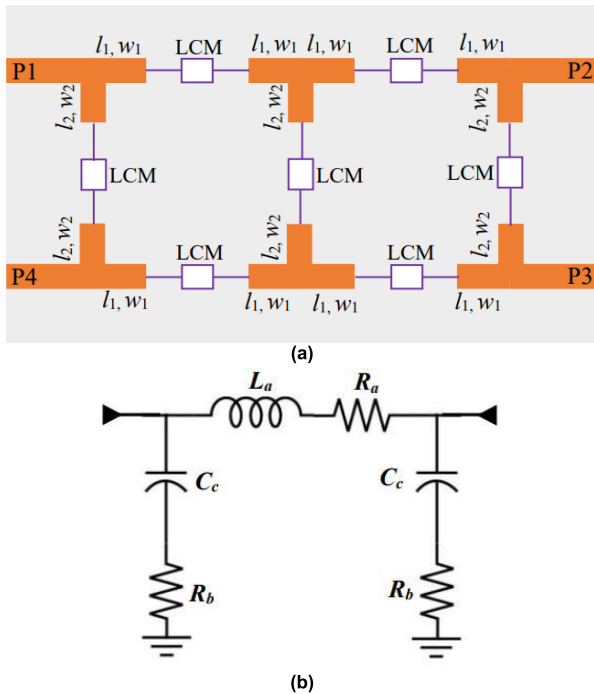
FIGURE 3. (a) Schematic of subnetworks of the BLCO; (b) Lumped-circuit model used for crossover simulation.

TABLE 1. Component values of proposed tunable BLCO.

Components	Values		
	Air	RO4360	RO3010
l_1 (mm)	11.9	11.9	11.9
w_1 (mm)	4.0	4.0	4.0
l_2 (mm)	11.9	11.9	11.9
w_2 (mm)	4.0	4.0	4.0
L_a (nH)	1.24	1.17	1.14
R_a (Ω)	0.8	0.16	0.01
C_c (pF)	0.145	0.373	0.52
R_b (Ω)	0.1	4.0	2.0098

C. LUMPED CIRCUIT MODEL ANALYSIS

Figure 3(a) shows the subnetworks of the proposed BLCO with seven RDCs. The dielectric channels are analyzed using a lumped circuit model (LCM), as depicted in Fig. 3(b). The Keysight Advanced Design System (ADS) simulator is employed to analyze the frequency tunability for various dielectric materials. The LCM component values are obtained from the S-parameters, calculated with CST Microwave Studio from 1 GHz to 2.6 GHz based on [37]. Three lumped-circuit models are developed for each dielectric channel: one for Roger's RO4360G2 ($\varepsilon_r = 6.02$), one for Roger's RO3010 ($\varepsilon_r = 10,2$), and another for the air-filled channels. The extracted component values for different dielectric materials are listed in Table 1.

To verify the frequency tunability of the proposed BLCO, a series of circuit simulations of the equivalent circuit model are performed as the channels are filled with RO4360G2,
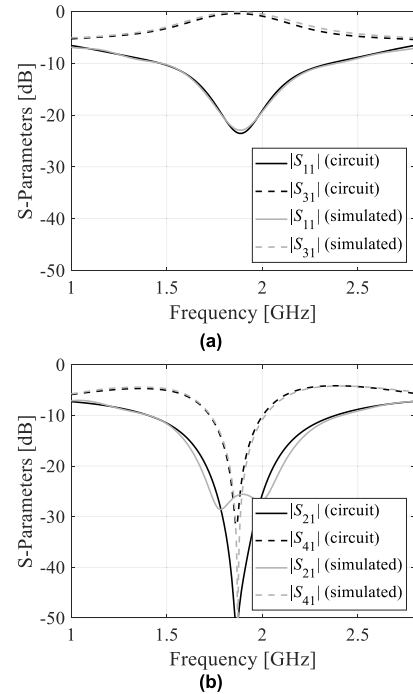

FIGURE 4. Circuit and EM simulated S-parameters of the proposed BLCO filled with one RDC of air: (a) $|S_{11}|$ and $|S_{31}|$, (b) $|S_{21}|$ and $|S_{41}|$.

RO3010, and air. The circuit and electromagnetic (EM) simulated S-parameters are compared for three different materials. Figure 4 shows the S-parameters for air-filled channels. Figure 5 depicts the S-parameters comparison for RO4360-filled channels. Similarly, Fig. 6 presents the S-parameters comparison for RO3010-filled channels.

The figures indicate an excellent agreement between the circuit and EM simulated frequency responses. The return losses and isolations are better than −20 dB for all dielectric materials. In addition, the fractional bandwidths for different materials are almost equal, considering a −15dB level for return loss and isolation. Analogously, the proposed concept can be extended for BLCO with 21 dielectric channels.

III. FABRICATION, RESULTS AND DISCUSSION

Two prototypes have been fabricated and experimentally demonstrated to validate the proposed concept. The prototypes are implemented on Roger's AD250C substrate with $h_s = 1.524$ mm, $\varepsilon_r = 2.5$, and $\tan \delta = 0.0014$. The first structure has one RDCs in each arm of the BLCO, whereas the second prototype contains three RDCs in each arm of the BLCO.

Figures 7(a) and (b) show the photographs of the fabricated BLCOs with seven and twenty-one RDCs, respectively. The RDCs are milled out on the top of the microstrip line, and filled with various dielectric materials. A two-port Rohde & Schwarz vector network analyzer is employed to perform the measurements, and the setup is shown in Fig. 7(c). The measurement is recorded upon filling the RDCs with air, Roger's RO4360G2 ($\varepsilon_r = 6.02$), and RO3010 ($\varepsilon_r = 10.2$) dielectric
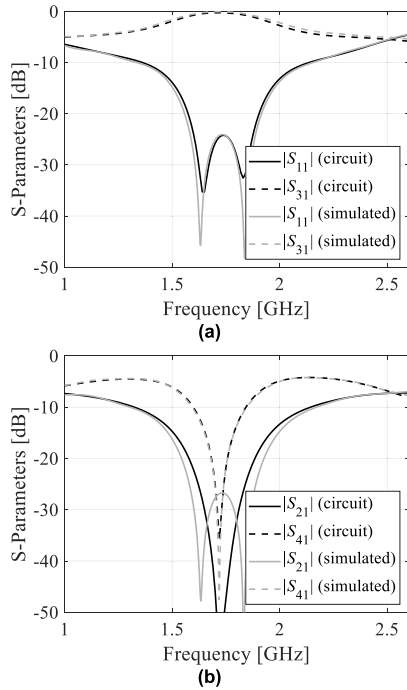
FIGURE 5. Circuit and EM simulated S-parameters of the proposed BLCO filled with one RDC of RO4360: (a) $|S_{11}|$ and $|S_{31}|$, (b) $|S_{21}|$ and $|S_{41}|$.
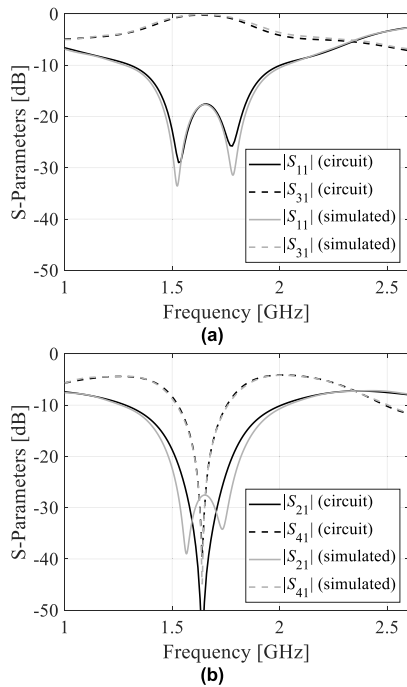

FIGURE 6. Circuit and EM simulated S-parameters of the proposed BLCO filled with one RDC of RO3010: (a) $|S_{11}|$ and $|S_{31}|$ (b) $|S_{21}|$ and $|S_{41}|$.

materials. After the RDCs are filled with dielectric materials, the copper tape covers the channels to restore connectivity.

A. RESULTS FOR BLCO WITH SEVEN RDCs

The EM simulated and measured S-parameters of the fabricated prototype of the tunable BLCO with seven RDCs have been shown in Figs. 8, 9, and 10. This prototype has only one
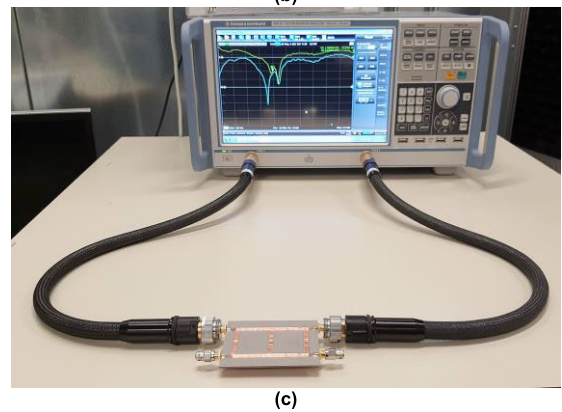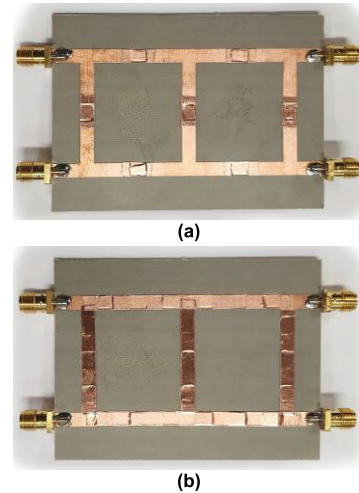

FIGURE 7. Fabricated prototypes of the proposed BLCO: (a) seven RDCs. (b) 21 RDCs, (c) measurement setup.

RDC in each arm of the BLCO. First, the BLCO is measured without any dielectric material, that is, with the air. Next, the RDC is filled with RO4630 ($\varepsilon_r = 6.02$) and RO3010 materials having ($\varepsilon_r = 10.2$). The operating frequency is shifted to 1.89 GHz by filling the RDC with air. The operating frequency is shifted to 1.71 GHz and 1.63 GHz by filling the RDC with RO 4630 and RO3010 materials, respectively. Therefore, the proposed BLCO with one RDC in each branch line can adjust its operating frequency from 1.63 GHz to 1.91 GHz, which corresponds to a 15.8-percent tuning range.

Referring to Fig. 8, it is found that the passband is centered at 1.88 GHz with the return loss and isolations greater than − 21 dB, whereas, the insertion loss at the through-port is less than 0.48 dB. The EM simulated and measured fractional bandwidths for a −15 dB level of return loss is greater than 29%. By filling the RDCs with RO4360 material, the passband is centered at 1.71GHz as depicted in Fig. 9. It is seen that the return loss and isolations are better than −19.5 dB, whereas, the insertion loss is found to be less than 0.41 dB. For −15 dB return loss, the EM simulated and tested fractional bandwidths are obtained as 27.5% and 29%, respectively. Figure 10 demonstrates that the passband is centered at 1.64GHz when the RDCs are filled with RO3010 material.
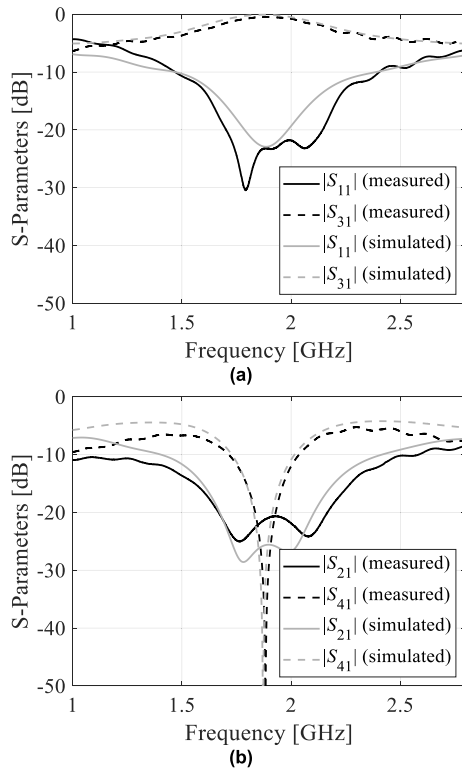
FIGURE 8. EM simulated and measured *S*-parameters of the BLCO-seven RDCs with air-filled: (a) $|S_{11}|$ and $|S_{31}|$, (b) $|S_{21}|$ and $|S_{41}|$.

FIGURE 9. EM simulated and measured *S*-parameters of the BLCO-seven RDCs with RO4360-filled: (a) $|S_{11}|$ and $|S_{31}|$, (b) $|S_{21}|$ and $|S_{41}|$.

The EM simulated and tested return loss and isolations are better than −16.9 dB and the through port insertion loss is
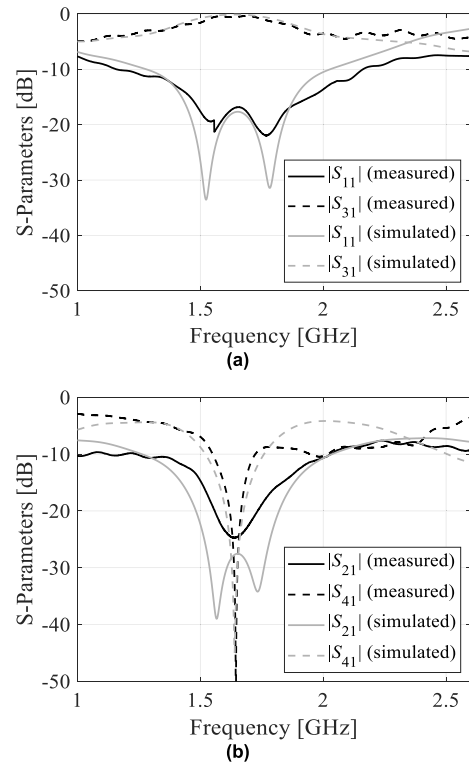

FIGURE 10. EM simulated and measured *S*-parameters of the BLCO-seven RDCs with RO3010-filled: (a) $|S_{11}|$ and $|S_{31}|$, (b) $|S_{21}|$ and $|S_{41}|$.
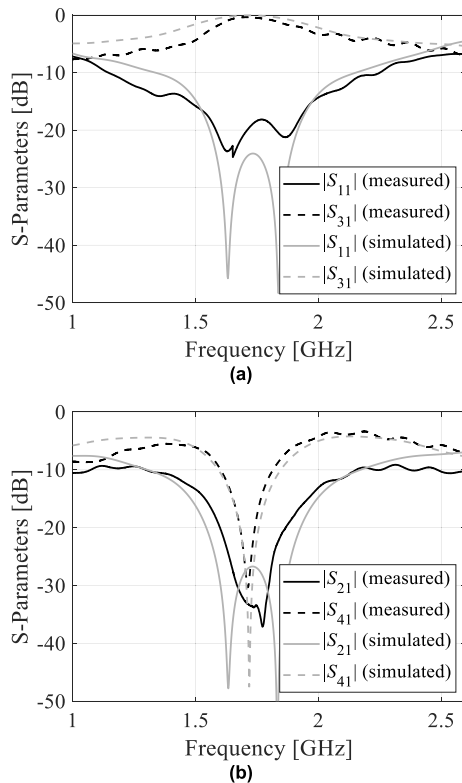
TABLE 2. Performance indicators of the proposed BLCO with one RDC in each branch line.

Parameters	Air		RO4360		RO3010	
	Sim.	Meas.	Sim.	Meas.	Sim.	Meas.
f_0 (GHz)	1.89	1.91	1.715	1.721	1.631	1.637
$|S_{11}|$ (dB)	22.9	23.2	24.2	19.5	17.96	16.91
$|S_{21}|$ (dB)	25.6	21.1	26.9	33.3	28.08	24.76
$|S_{31}|$ (dB)	0.09	0.48	0.06	0.41	0.11	0.57
$|S_{41}|$ (dB)	33.9	38.1	47.5	28.5	43.67	39.24
FWB (%)	22.1	29.8	27.4	29	28.2	29.5

obtained as less than 0.57 dB. The fractional bandwidths are found to be greater than 28%, considering a −15dB level return loss. The performance indicators of the proposed tunable BLCO with one RDC in each arm are shown in Table 2. Hence, it is noted that the passband frequency can be tuned to lower values by using dielectric materials of higher permittivity.

B. RESULTS FOR BLCO WITH TWENTY ONE RDCs
Figure 7(b) shows the fabricated prototype of the tunable BLCO with 21 RDCs. For the first measurement (case-1), All RDCs are packed with air, RO4360, and RO3010 materials, and the corresponding S-parameters are recorded. The EM simulation and measured S-parameters are illustrated in Figs. 11, 12, and 13. The passband is centered at 2.05GHz, 1.56GHz, and 1.41GHz when the RDCs are filled with air, RO4360, and RO3010, respectively. Hence, the proposed
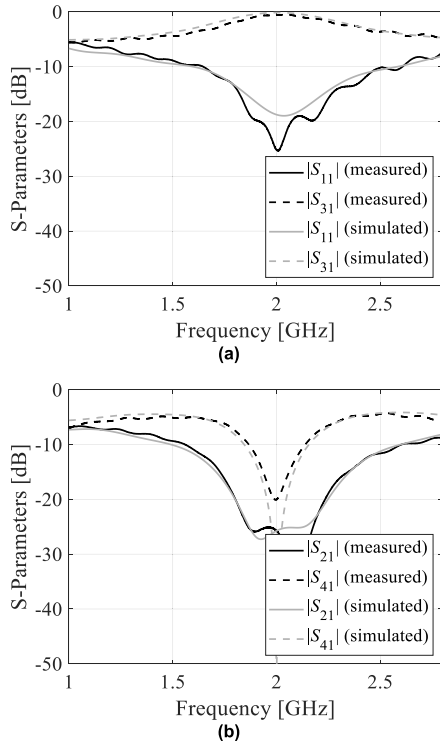
FIGURE 11. EM simulated and measured S-parameters of the BLCO-twenty-one RDCs with air-filled (a) $|S_{11}|$ and $|S_{31}|$, (b) $|S_{21}|$ and $|S_{41}|$.
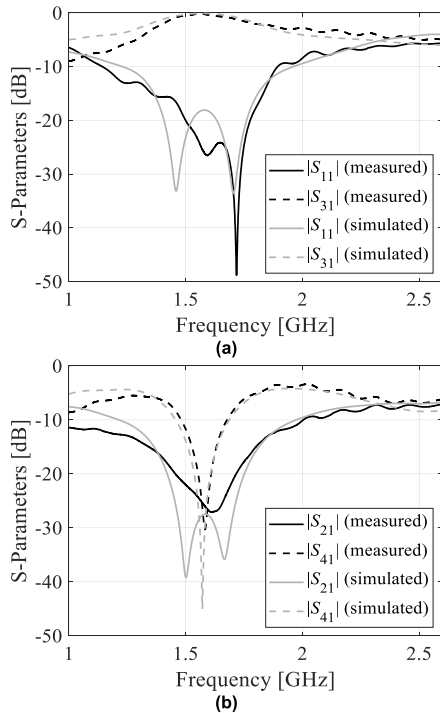
FIGURE 12. EM simulated and measured S-parameters of the BLCO-twenty-one RDCs with RO4360-filled: (a) $|S_{11}|$ and $|S_{31}|$, (b) $|S_{21}|$ and $|S_{41}|$.

BLCO is tuned from 1.41 GHz to 2.05 GHz, which corresponds to a 36.9-percent tuning range. From Fig. 11, it is obtained that the return loss and isolations are greater than

TABLE 3. Performance indicators of the proposed BLCO with three RDCs in each branch line: case-1.

Parameters	Air		RO4360		RO3010	
	Sim.	Meas.	Sim.	Meas.	Sim.	Meas.
f_0 (GHz)	2.04	2.05	1.56	1.57	1.41	1.42
$|S_{11}|$ (dB)	18.96	21.24	18.34	24.6	13.21	17.45
$|S_{21}|$ (dB)	25.22	28.31	28.2	25.3	28.78	26.11
$|S_{31}|$ (dB)	0.16	0.53	0.11	0.32	0.35	0.90
$|S_{41}|$ (dB)	21.3	17.96	29.7	23.45	35.19	28.22
FWB (%)	18.23	21.56	28.65	30.3	31.2	26.7

TABLE 4. Performance indicators of the proposed BLCO with three RDCs in each branch line: case-2.

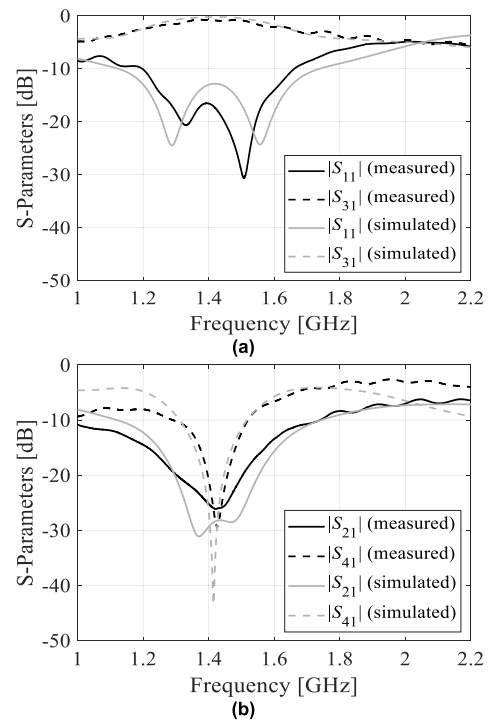| Parameters	RO4360		RO3010	
	Sim.	Meas.	Sim.	Meas.
f_0 (GHz)	1.68	1.687	1.54	1.55
$|S_{11}|$ (dB)	34.63	40.43	21.16	22.18
$|S_{21}|$ (dB)	26.94	19.29	27.64	22.74
$|S_{31}|$ (dB)	0.06	0.12	0.07	0.49
$|S_{41}|$ (dB)	48	23.73	39.24	21.76
FWB (%)	25.8	34.85	27.5	27.6

FIGURE 13. EM simulated and measured S-parameters of the BLCO-twenty-one RDCs with RO3010-filled: (a) $|S_{11}|$ and $|S_{31}|$, (b) $|S_{21}|$ and $|S_{41}|$.

−17.9 dB at the passband, whereas the insertion loss is less than 0.53 dB. A fractional bandwidth of 21% is obtained considering a −15dB level of return loss. Referring to Fig. 12, the return loss and isolations are better than −18.3 dB and the insertion loss is less than 0.32 dB. For a −15 dB level of return loss, the fractional bandwidth is computed as 28%. As depicted in Fig. 13, the return loss and isolations are greater than −13.2 dB and the insertion loss is less than 0.9 dB.

TABLE 5. Performance comparison of SIW Self-diplexing antennas.

Ref.	Freq. (GHz)	$|S_{11}|$ (dB)	$|S_{21}|$ (dB)	$|S_{31}|$ (dB)	$|S_{41}|$ (dB)	FBW (%)	Passband
[6]	5.50	>13	>12	<0.5	>12	12.7	SFB
[7]	1.0	>16	>15	<0.97	>15	55	SFB
[8]	11.6	>10	>37	<2	>37	62.7	SFB
[10]	2.03	>18	>22	<1.0	>22	29.5	SFB
[11]	2.5	>20	>20	<0.5	>20	23.0	SFB
[12]	1.0	>10	>10	<0.5	>10	22	SFB
[13]	2.5	>20	>20	<0.5	>20	22	SFB
[14]	3.0	>27	>22	<0.3	>22	30	SFB
[15]	0.9/2.45	>20	>20	<1.34	>20	–	DFB
[16]	1.0/2.3	>20	>20	<0.57	>20	6.5	DFB
[17]	2.4/5.0	>20	>30	<1.0	>30	4.15	DFB
[18]	0.78/1.22	>20	>20	<0.65	>20	11	DFB
[19]	1.75/4.06	>10	>20	<0.6	>20	7.5	DFB
[21]	0.9/5.4	>20	>20	<0.67	>20	6.7	DFB
[38]	1.29 − 2.06	>20	>20	0.59 − 1.22	>20	1.95 − 3.1	Tunable
[39]	2.2 − 5.0	>19	>15	0.93 − 1.97	>15	1.8 − 4.7	Tunable
Design I	**1.63 − 1.93**	**17.9 − 24.2**	**21.1 − 24.7**	**0.06 − 0.57**	**28.5 − 47.5**	**27 − 29**	Tunable
Design II	**1.41 − 2.05**	**17.4 − 21.2**	**26.1 − 28.3**	**0.11 − 0.90**	**17.9 − 35.1**	**21 − 28**	Tunable

SFB: Single fixed band, DFB: Dual fixed band

FIGURE 14. EM simulated and measured S-parameters of the BLCO-twenty-one RDCs with air-filled between two RO4360-filled RDCs in each arm: (a) $|S_{11}|$ and $|S_{31}|$, (b) $|S_{21}|$ and $|S_{41}|$.
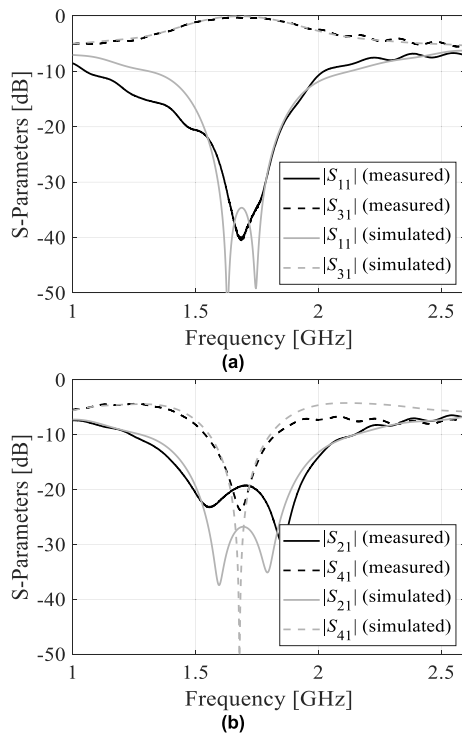

FIGURE 15. EM simulated and measured S-parameters of the BLCO-twenty-one RDCs with air-filled between two RO3010-filled RDCs in each arm: (a) $|S_{11}|$ and $|S_{31}|$, (b) $|S_{21}|$ and $|S_{41}|$.

A fractional bandwidth of 26% is obtained for −13 dB return loss. The performances of EM simulation and measurements for air, RO4360, and RO3010 are shown in Table 3.

In the second measurement (case-2), the middle RDC of each arm is kept empty and two adjacent RDCs are filled with RO4360 and RO3010 materials. The corresponding S-parameters are obtained and compared with the EM simulated one as depicted in Figs. 14 and 15. Figure 14 indicates
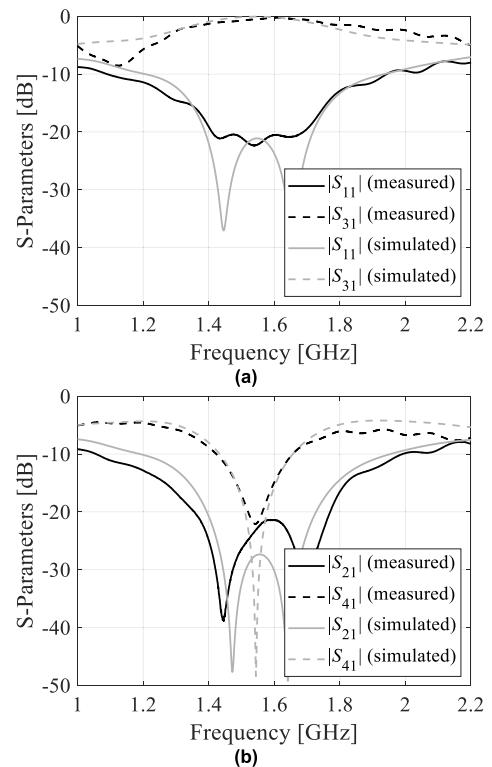
that the return loss and isolations are greater than −19.2 dB, whereas the insertion loss is less than 0.2 dB. For a −15 dB return loss, the fractional bandwidth is obtained more than 25%. Referring to Fig. 15, the return loss and isolations are found to be better than −21.1 dB and the insertions loss is less than 0.49 dB. A fractional bandwidth of 27% is recorded

considering a −15dB return loss. The EM simulated and tested performances are compared as shown in Table 4.

Table 5 shows a comparative study to demonstrate the superiority of the proposed reconfigurable crossover over the previously reported crossovers. Compared to [6], [7], [8], [9], [10], [11], [12], [13], [14], [15], [16], [17], [18], [19], [20], [21], [38], and [39], the proposed crossover exhibits minimal insertion loss throughout the tuning range. When compared to [6], [7], [8], [9], [10], [11], [12], [13], [14], [15], [16], [17], [18], [19], [20], [21], [38], and [39], the proposed crossover achieves excellent fractional bandwidth, isolation, and return loss. In addition, while the proposed work and earlier works in [38] and [39] show frequency tunable crossovers, the crossovers reported in [6], [7], [8], [9], [10], [11], [12], [13], [14], [15], [16], [17], [18], [19], [20], and [21] demonstrate single/dual-band operation. In [38] and [39], crossovers provide wide tuning range by using varactor diodes that results in major drawbacks such as low power-handling levels and lack of compatibility required for wearable components. To overcome these drawbacks, a passive reconfigurable technique is used in the this work. Moreover, the frequency tuning range can be increased by using dielectric materials with higher permittivity. In comparison to [38] and [39], the proposed crossover features low insertion loss, high isolation, and high fractional bandwidth. The proposed reconfigurable crossover is also validated using an equivalent lumped circuit model.

IV. CONCLUSION

This paper describes a simple passive reconfiguration technique for tuning the operating frequency of a branch-line crossover (BLCO). The basic idea is to fill rectangular dielectric channels (RDCs) that have been previously arranged with either air or materials of different relative permittivity. To estimate the tunability range of the operating frequency, two crossover configurations (one RDC and three RDCs in each branch line) have been realized. The accumulation of RDCs packed with different materials in the branch lines changes the effective permittivity of the dielectric medium, causing the operating frequency to alter. Full-wave electromagnetic simulations are used to optimize the size and position of the RDCs in order to achieve maximum tunability range while maintaining reasonable bandwidth. To analyze the working principle of the proposed technique, a lumped circuit model (LCM) has been developed. Two crossover prototypes are realized, fabricated, and experimentally demonstrated to validate computational models. The agreement between EM-simulated and measured responses is excellent. However, due to fabrication tolerance, connector loss, and conductor surface precision, small differences have been observed between EM simulations and experimental results. Notwithstanding, it has been corroborated that the first prototype (containing one RDC in each branch line) exhibits a frequency tuning range of 15.8%, whereas the second prototype (containing three RDCs in each branch line) features a tuning range of 36.9%.

REFERENCES

[1] H. Y. Yang and N. G. Alexopoulos, "Basic blocks for high-frequency interconnects: Theory and experiment," *IEEE Trans. Microw. Theory Techn.*, vol. MTT-36, no. 8, pp. 1258–1264, Aug. 1988.

[2] T. Becks and I. Wolff, "Analysis of 3-D metallization structures by a full-wave spectral-domain technique," *IEEE Trans. Microw. Theory Techn.*, vol. 40, no. 12, pp. 2219–2227, Dec. 1992.

[3] T.-S. Horng, "A rigorous study of microstrip crossovers and their possible improvements," *IEEE Trans. Microw. Theory Techn.*, vol. 42, no. 9, pp. 1802–1806, Sep. 1994.

[4] J. J. Yao, "Nonstandard hybrid and crossover design with branch-line structures," *IEEE Trans. Microw. Theory Techn.*, vol. 58, no. 12, pp. 3801–3808, Dec. 2010.

[5] J.-J. Yao, C. Lee, and S.-P. Yeo, "Microstrip branch-line couplers for crossover application," *IEEE Trans. Microw. Theory Techn.*, vol. 59, no. 1, pp. 87–92, Jan. 2011.

[6] A. M. Abbosh, "Planar wideband crossover with distortionless response using dual-mode microstrip patch," *Microw. Opt. Technol. Lett.*, vol. 54, no. 9, pp. 2077–2079, Jun. 2012.

[7] C. W. Tang, K. C. Lin, and W. C. Chen, "Analysis and design of compact and wide-passband planar crossovers," *IEEE Trans. Microw. Theory Techn.*, vol. 62, no. 12, pp. 2975–2982, Dec. 2014.

[8] D. Sun and J. Xu, "A wide band and high isolation microstrip line crossover using microstrip to ridge waveguide transitions," *Microw. Opt. Technol. Lett.*, vol. 58, no. 5, pp. 1148–1150, May 2016.

[9] S. P. Yeo and N. Deng, "Multi-section branch-line couplers for crossover application," *Microw. Opt. Technol. Lett.*, vol. 59, no. 7, pp. 1625–1629, Jul. 2017.

[10] B. Zhang, C. Yu, Y. Wu, and Y. Liu, "Compact wideband filtering microstrip crossover with separated operating frequencies," *Microw. Opt. Technol. Lett.*, vol. 60, no. 3, pp. 731–735, Mar. 2018.

[11] T. Kim, J. Lee, and J. Choi, "Analysis and design of miniaturized multi-section crossover with open stubs," *Microw. Opt. Technol. Lett.*, vol. 57, no. 11, pp. 2673–2677, Nov. 2015.

[12] M. A. Antoniades, B. Henin, and A. Abbosh, "A compact crossover using NRI-TL metamaterial lines," in *Proc. IEEE Int. Symp. Antennas Propag.*, Chicago, IL, USA, Jul. 2012, pp. 1–2.

[13] T. Kim and J. Choi, "Miniaturized multi-section crossover with open stub," in *Proc. IEEE Int. Symp. Antennas Propag. USNC/URSI Nat. Radio Sci. Meeting*, Vancouver, BC, Canada, Jul. 2015, pp. 1044–1045.

[14] K. Al Shamaileh, O. Hussein, N. Dib, A. Nosrati, and V. Devabhaktuni, "Multi-section branch-line crossover/coupler optimization for wideband applications and higher-order harmonics suppression," *AEU, Int. J. Electron. Commun.*, vol. 122, Jul. 2020, Art. no. 153269.

[15] S.-Y. Hsieh and P.-L. Chi, "Miniaturized dual-band composite right/left-handed crossover," in *Proc. Asia–Pacific Microw. Conf. Proc. (APMC)*, Nov. 2013, pp. 282–284.

[16] F. Lin, Q.-X. Chu, and S. W. Wong, "Dual-band planar crossover with two-section branch-line structure," *IEEE Trans. Microw. Theory Techn.*, vol. 61, no. 6, pp. 2309–2316, Jun. 2013.

[17] I. S. Krishna, R. K. Barik, and S. S. Karthikeyan, "Analysis and design of a planar crossover for dual-frequency applications," in *Proc. 14th IEEE India Council Int. Conf. (INDICON)*, Roorkee, India, Dec. 2017, pp. 1–5.

[18] W. Feng, Y. Zhao, and W. Che, "Dual-band crossover using loaded coupled lines," in *Proc. IEEE Int. Conf. Comput. Electromagn. (ICCEM)*, Chengdu, China, Mar. 2018, pp. 1–2.

[19] H. Shahi, J. Mazloum, and M. Bayat, "Differential-to-single-ended crossover based on dumbbell-shaped defected ground resonators for dual-band applications," *Int. J. RF Microw. Comput.-Aided Eng.*, vol. 31, no. 6, Jun. 2021, Art. no. e22666.

[20] H. Ren, J. Shao, M. Zhou, B. Arigong, J. Ding, and H. Zhang, "Novel design of multiband branch-line coupler using multiband transmission lines," *Microw. Opt. Technol. Lett.*, vol. 56, no. 12, pp. 2841–2845, Dec. 2014.

[21] I. S. Krishna, R. K. Barik, and S. S. Karthikeyan, "A dual-band crossover using cross-shaped microstrip line for small and large band ratios," *Int. J. Microw. Wireless Technol.*, vol. 9, no. 8, pp. 1629–1635, Oct. 2017.

[22] M. R. Khan, G. J. Hayes, S. Zhang, M. D. Dickey, and G. Lazzi, "A pressure responsive fluidic microstrip open stub resonator using a liquid metal alloy," *IEEE Microw. Wireless Compon. Lett.*, vol. 22, no. 11, pp. 577–579, Nov. 2012.

[23] G. Mumcu, A. Dey, and T. Palomo, "Frequency-agile bandpass filters using liquid metal tunable broadside coupled split ring resonators," *IEEE Microw. Wireless Compon. Lett.*, vol. 23, no. 4, pp. 187–189, Apr. 2013.

[24] D. L. Diedhiou, R. Sauleau, and A. V. Boriskin, "Microfluidically tunable microstrip filters," *IEEE Trans. Microw. Theory Techn.*, vol. 63, no. 7, pp. 2245–2252, Jul. 2015.

[25] W.-J. Zhou, H. Tang, and J.-X. Chen, "Novel microfluidically tunable differential dual-mode patch filter," *IEEE Microw. Wireless Compon. Lett.*, vol. 27, no. 5, pp. 461–463, May 2017.

[26] T. Palomo and G. Mumcu, "Microfluidically reconfigurable microstrip line combline filters with wide frequency tuning capabilities," *IEEE Trans. Microw. Theory Techn.*, vol. 65, no. 10, pp. 3561–3568, Oct. 2017.

[27] E. González-Carvajal and G. Mumcu, "Frequency and bandwidth tunable mm-wave hairpin bandpass filters using microfluidic reconfiguration with integrated actuation," *IEEE Trans. Microw. Theory Techn.*, vol. 68, no. 9, pp. 3756–3768, Sep. 2020.

[28] M. Li and N. Behdad, "Fluidically tunable frequency selective/phase shifting surfaces for high-power microwave applications," *IEEE Trans. Antennas Propag.*, vol. 60, no. 6, pp. 2748–2759, Jun. 2012.

[29] B. J. Lei, A. Zamora, T. F. Chun, A. T. Ohta, and W. A. Shiroma, "A wideband, pressure-driven, liquid-tunable frequency selective surface," *IEEE Microw. Wireless Compon. Lett.*, vol. 21, no. 9, pp. 465–467, Sep. 2011.

[30] D. Rodrigo, L. Jofre, and B. A. Cetiner, "Circular beam-steering reconfigurable antenna with liquid metal parasitics," *IEEE Trans. Antennas Propag.*, vol. 60, no. 4, pp. 1796–1802, Apr. 2012.

[31] A. J. King, J. F. Patrick, N. R. Sottos, S. R. White, G. H. Huff, and J. T. Bernhard, "Microfluidically switched frequency-reconfigurable slot antennas," *IEEE Antennas Wireless Propag. Lett.*, vol. 12, pp. 828–831, 2013.

[32] A. Singh, I. Goode, and C. E. Saavedra, "A multistate frequency reconfigurable monopole antenna using fluidic channels," *IEEE Antennas Wireless Propag. Lett.*, vol. 18, no. 5, pp. 856–860, May 2019.

[33] S. De, S. K. Koul, and K. K. Samanta, "Dielectric rod loaded tunable substrate integrated waveguide slot antenna," *IET Microw., Antennas Propag.*, vol. 16, nos. 2–3, pp. 163–173, Feb. 2022.

[34] M. M. Shirkolaei and M. Aslinezhad, "Substrate integrated waveguide filter based on the magnetized ferrite with tunable capability," *Microw. Opt. Technol. Lett.*, vol. 63, no. 4, pp. 1120–1125, Apr. 2021.

[35] M. M. Shirkolaei and M. Jafari, "A new class of wideband microstrip falcate patch antennas with reconfigurable capability at circular-polarization," *Microw. Opt. Technol. Lett.*, vol. 62, no. 12, pp. 3922–3927, Dec. 2020.

[36] F. Moayyed, H. R. D. Oskouei, and M. Mohammadi Shirkolaei, "High gain and wideband multi-stack multilayer anisotropic dielectric antenna," *Prog. Electromagn. Res. Lett.*, vol. 99, pp. 103–109, 2021.

[37] M. Brown, I. Goode, and C. E. Saavedra, "Lumped-element circuit modelling of microfluidic channels in microstrip transmission lines," in *Proc. 16th IEEE Int. New Circuits Syst. Conf. (NEWCAS)*, Montreal, QC, Canada, Jun. 2018, pp. 31–34.

[38] F. Lin, S. W. Wong, and Q.-X. Chu, "Compact design of planar continuously tunable crossover with two-section coupled lines," *IEEE Trans. Microw. Theory Techn.*, vol. 62, no. 3, pp. 408–415, Mar. 2014.

[39] Q. Cui and F. Lin, "Continuously tunable crossover based on HMSIW," *Electron. Lett.*, vol. 53, no. 24, pp. 1582–1583, Nov. 2017.

RUSAN KUMAR BARIK (Member, IEEE) received the B.Tech. degree in electronic and communication engineering from the Biju Patnaik University of Technology, Rourkela, India, in 2012, and the M.Tech. degree in communication systems design and the Ph.D. degree in electronics engineering from the Indian Institute of Information Technology, India, in 2015 and 2018, respectively. In 2018, he joined the Department of Electronics and Communication Engineering, Christ University, Bengaluru, India, as an Assistant Professor. In 2019, he joined the Department of Electrical and Electronic Engineering, Southern University of Science and Technology, Shenzhen, China, as a Postdoctoral Researcher. He is currently a Postdoctoral Researcher with the Engineering Optimization and Modeling Center (EOMC), Department of Electrical Engineering, Reykjavik University, Iceland. His research interests include multiband microwave devices, SIW components, surrogate-based modeling, and optimization.

SLAWOMIR KOZIEL (Fellow, IEEE) received the M.Sc. and Ph.D. degrees in electronic engineering from the Gdańsk University of Technology, Poland, in 1995 and 2000, respectively, and the M.Sc. degree in theoretical physics and the M.Sc. and Ph.D. degrees in mathematics from the University of Gdańsk, Poland, in 2000, 2002, and 2003, respectively. He is currently a Professor with the Department of Engineering, Reykjavik University, Iceland. His research interests include CAD and modeling of microwave and antenna structures, simulation-driven design, surrogate-based optimization, space mapping, circuit theory, analog signal processing, evolutionary computation, and numerical analysis.

EIRÍKUR BERNHARÐSSON received the B.Sc. degree in mechatronics engineering from Reykjavik University, in 2022, where he is currently pursuing the B.Sc. degree in computer science. He is an Assistant Researcher for Prof. Slawomir Koziel and a Documentarian and Rover Operator on the NASA-funded RAVEN Project led by The University of Arizona. His research interests include robotics and automation, computer vision, control theory, and learning-based models.

• • •